

1 Supplemental Material for:

2 Subseasonal-to-seasonal forecast skill in the California Current  
3 System and its connection to coastal Kelvin waves  
4

5  
6 Dillon J. Amaya<sup>1</sup>, Michael G. Jacox<sup>1,2</sup>, Juliana Dias<sup>1</sup>, Michael A. Alexander<sup>1</sup>, Kristopher B.  
7 Karnauskas<sup>3,4</sup>, James D. Scott<sup>1,3</sup>, and Maria Gehne<sup>1,3</sup>

8  
9 **<sup>1</sup>Physical Science Laboratory, Earth System Research Laboratory, National Oceanic and  
10 Atmospheric Administration**

11 **<sup>2</sup>Environmental Research Division, Southwest Fisheries Science Center, National Oceanic  
12 and Atmospheric Administration**

13 **<sup>3</sup>Cooperative Institute for Research in Environmental Sciences, University of Colorado  
14 Boulder**

15 **<sup>4</sup>Department of Atmospheric and Oceanic Sciences, University of Colorado Boulder**

16  
17  
18  
19  
20 Corresponding author: Dillon J. Amaya, [dillon.amaya@noaa.gov](mailto:dillon.amaya@noaa.gov), 816-916-8348

21  
22  
23

24

## 25 **Tide gauge measurements**

26 The tide gauge data used for verifying GLORYS are maintained by the Joint Archive for  
27 Sea Level (JASL), which is a partnership between the University of Hawaii Sea Level Center  
28 (UHSLC) and the National Centers for Environmental Information (NCEI). Here, we utilize the  
29 Research Quality Data Set (RQDS) available at: <http://ilikai.soest.hawaii.edu/UHSLC/jasl.html>.

30 These observations are not assimilated in GLORYS and therefore offer an independent metric by  
31 which to verify the reanalysis. The monthly mean GLORYS and tide gauge anomalies used for  
32 Figure 2 and Table 1 are relative to a long-term monthly mean climatology from 1993-2018. The  
33 daily mean GLORYS and tide gauge anomalies used for Table 1 were calculated by removing the  
34 first three harmonics of the seasonal cycle over the same time period. Correlation significance  
35 between the two data sets was determined using a Student's t-test with a 95% confidence interval.

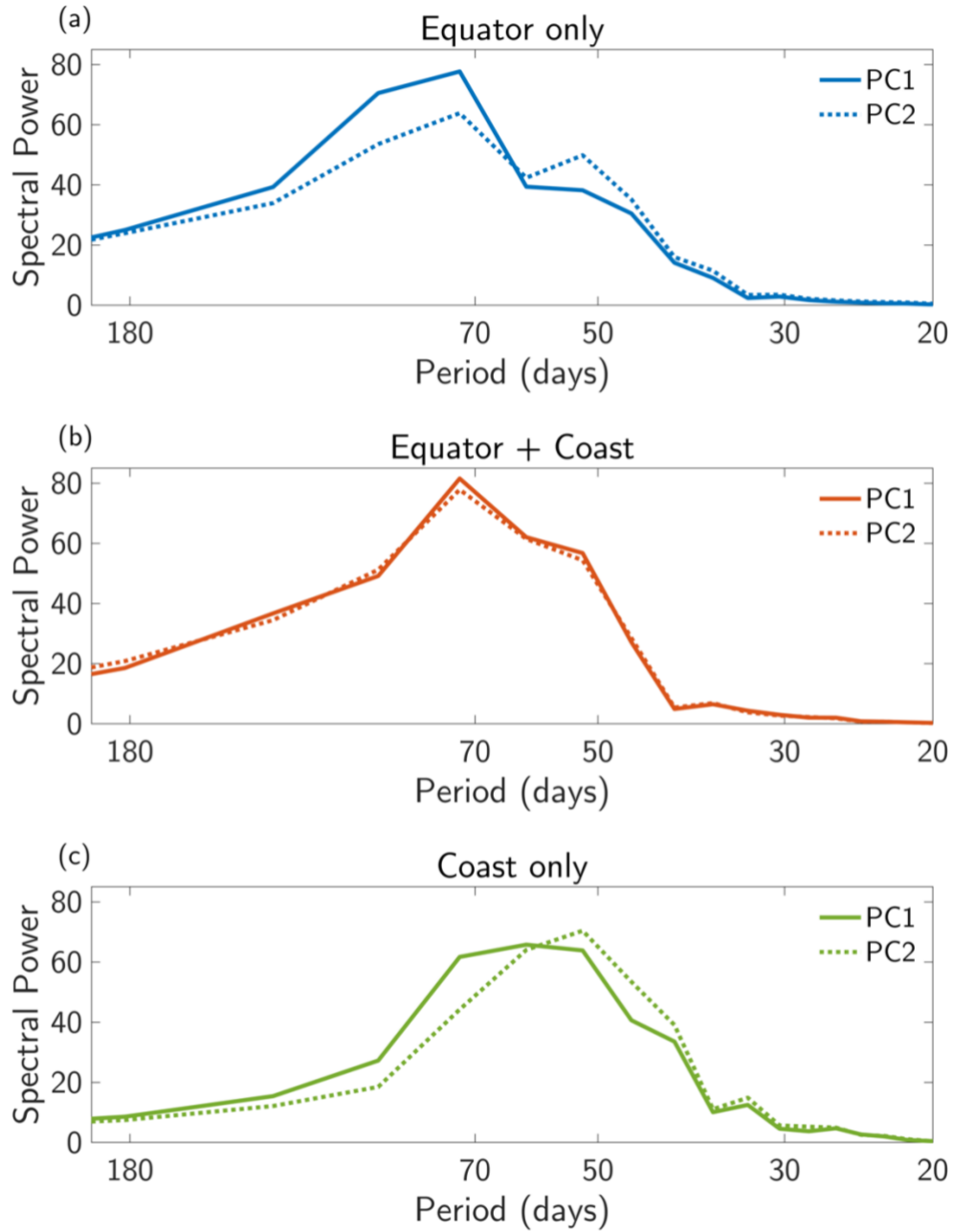
36

## 37 **Kelvin wave index phase composites**

38 In order to validate that each pair of EOFs discussed in Section 3.2 represent KWs  
39 propagating along our pathway, we define the phase relationship at time step  $t$  between each set of  
40 PC1 and PC2 as:

$$41 \quad \text{Phase}(t) = \tan^{-1} \left( \frac{PC2(t)}{PC1(t)} \right) \quad (2)$$

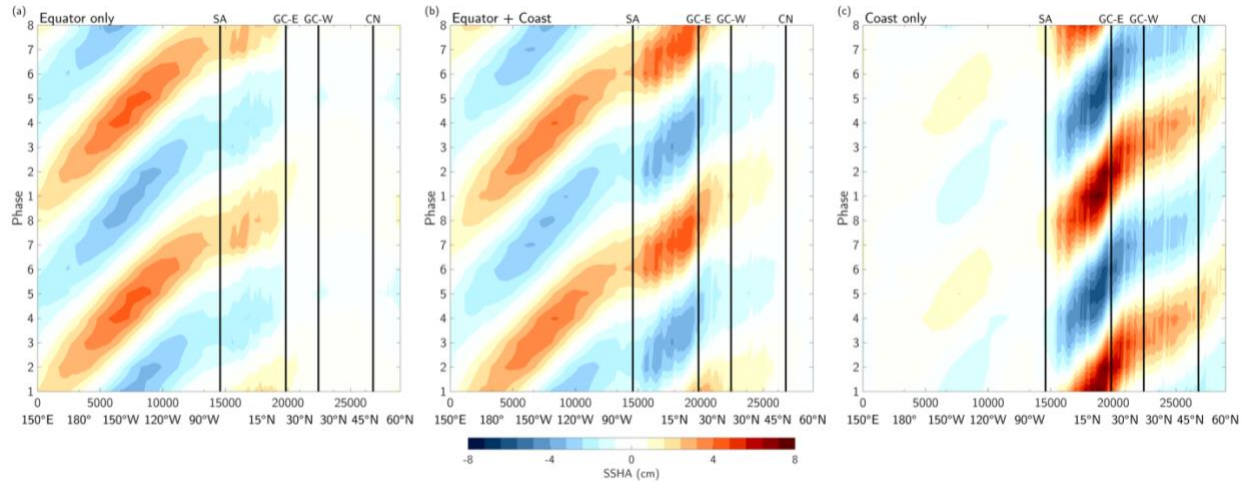
42 The resulting timeseries depict phases ranging from  $0^\circ$ - $360^\circ$  that describe the physical location of  
43 the propagating waves as they move through time. Analogous to the various MJO indices (e.g.,  
44 Kiladis et al. 2014), these phases can be further subdivided into eight equal  $45^\circ$  segments. We then  
45 compute composites of GLORYS filtered SSH anomalies, compositing when each index is greater  
46 than 1 in each phase (Figure S2).



47

48 **Figure S1** Power spectra of each PC1 and PC2 pairing from the (a) Equator only, (b) Equator +  
 49 Coast, and (c) Coast only EOF analyses.

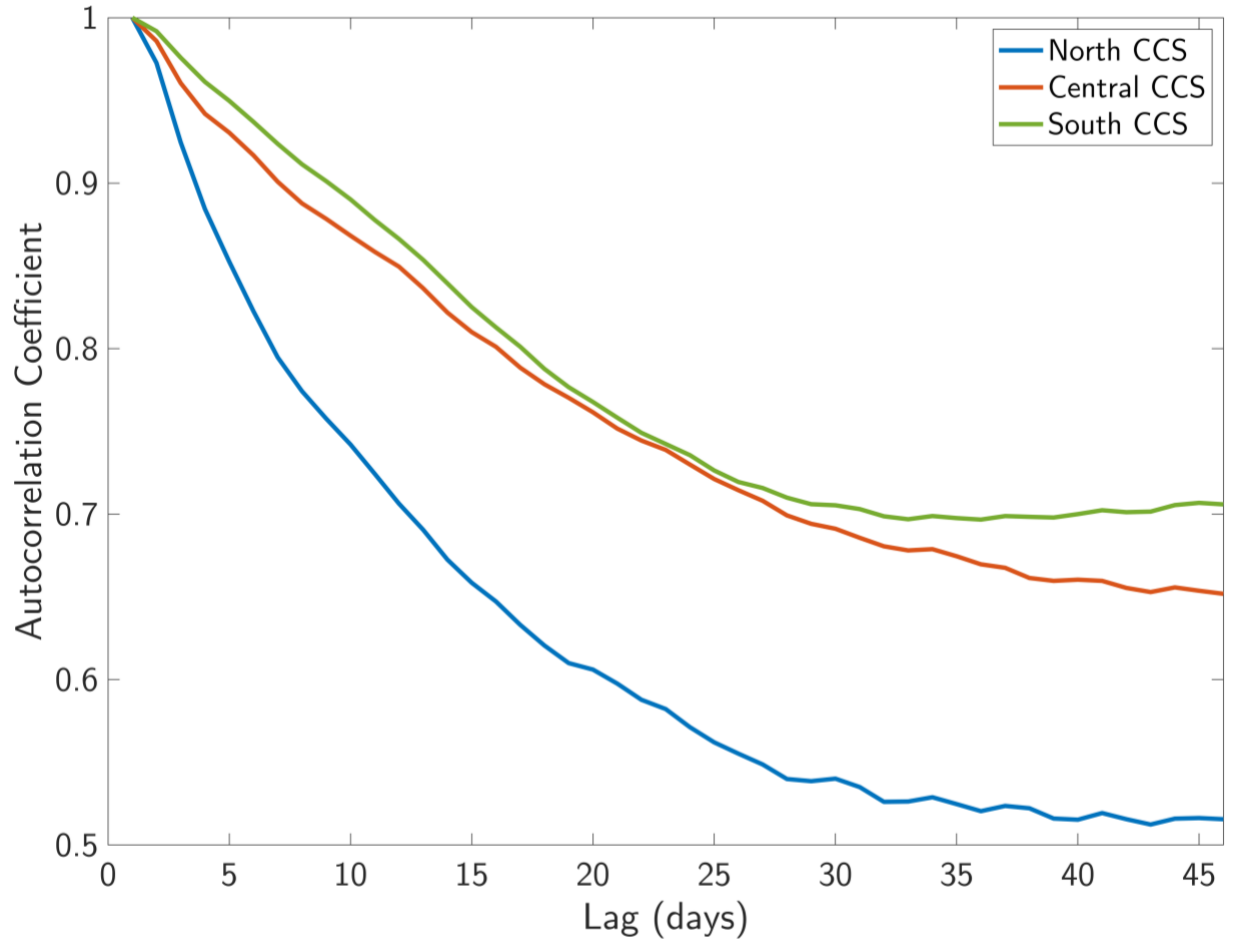
50



51

52 **Figure S2** Wavenumber and time filtered SSH anomalies (cm) composited on the eight phases of  
 53 the (a) E-KW index, (b) EC-KW index, and (c) C-KW index when the amplitude of each respective  
 54 index was also greater than or equal to 1. Patterns were repeated along the y-axis for clarity. Upper  
 55 x-axis marks the distance along the pathway in kilometers. Lower x-axis marks the approximate  
 56 latitude/longitude coordinates at select locations along the path.

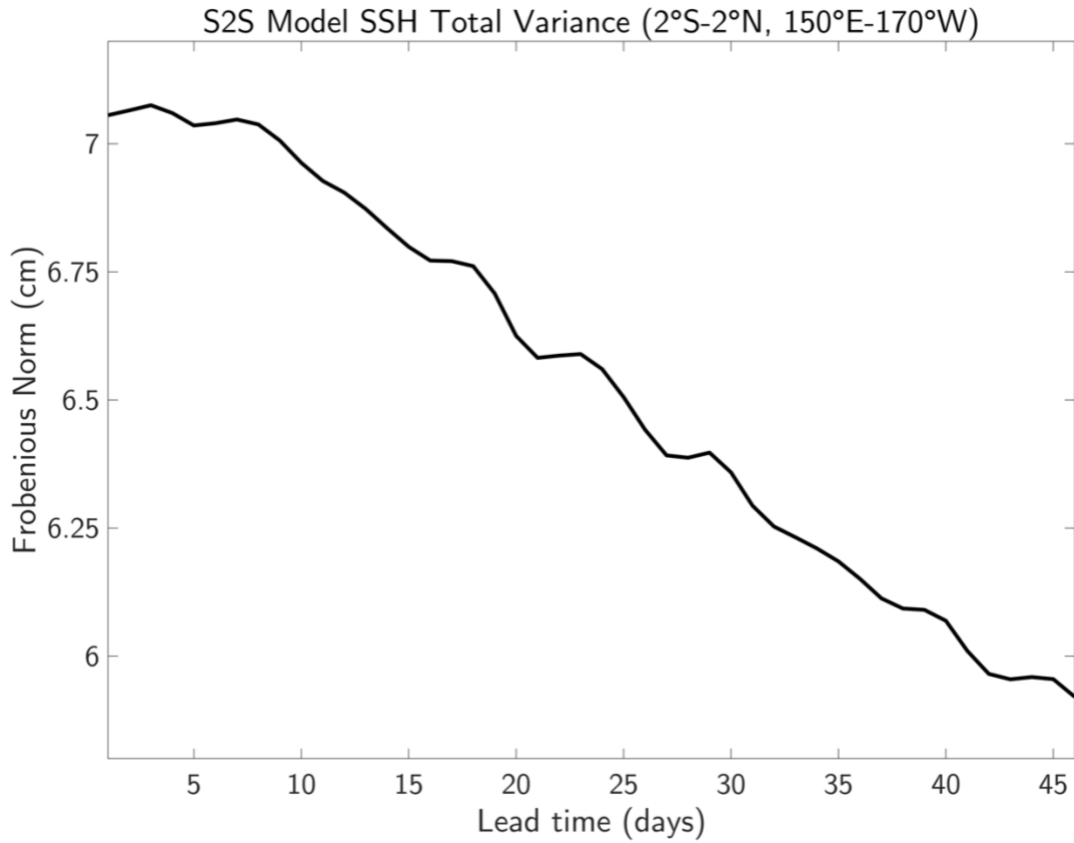
57



58

59 **Figure S3** Autocorrelation functions of unfiltered GLORYS SSH anomalies averaged in the North  
60 CCS (blue), Central CCS (orange), and South CCS (green).

61



62

63 **Figure S4** The Frobenius Norm (i.e., the total variance) of S2S SSH anomalies as a function of

64 lead time in the domain (2°S-2°N, 150°E-170°W).